AIP | Journal of Applied Physics

GaSb quantum rings in GaAs/AlxGa1−xAs quantum wells

P. D. Hodgson, M. Hayne, A. J. Robson, Q. D. Zhuang, and L. Danos

Citation: Journal of Applied Physics **119**, 044305 (2016); doi: 10.1063/1.4940880
View online: http://dx.doi.org/10.1063/1.4940880
View Table of Contents: http://scitation.aip.org/content/aip/journal/jap/119/4?ver=pdfcov
Published by the AIP Publishing

GaSb quantum rings in GaAs/$Al_xGa_{1-x}As$ quantum wells

P. D. Hodgson,[1,a)] M. Hayne,[1] A. J. Robson,[1] Q. D. Zhuang,[1] and L. Danos[2]
[1]*Department of Physics, Lancaster University, Lancaster LA1 4YB, United Kingdom*
[2]*Department of Chemistry, Lancaster University, Lancaster LA1 4YB, United Kingdom*

(Received 24 July 2015; accepted 15 January 2016; published online 29 January 2016)

We report the results of continuous and time-resolved photoluminescence measurements on type-II GaSb quantum rings embedded within GaAs/$Al_xGa_{1-x}As$ quantum wells. A range of samples were grown with different well widths, compensation-doping concentrations within the wells, and number of quantum-ring layers. We find that each of these variants have no discernible effect on the radiative recombination, except for the very narrowest (5 nm) quantum well. In contrast, single-particle numerical simulations of the sample predict changes in photoluminescence energy of up to 200 meV. This remarkable difference is explained by the strong Coulomb binding of electrons to rings that are multiply charged with holes. The resilience of the emission to compensation doping indicates that multiple hole occupancy of the quantum rings is required for efficient carrier recombination, regardless of whether these holes come from doping or excitation. [http://dx.doi.org/10.1063/1.4940880]

I. INTRODUCTION

GaSb quantum dots (QDs) and quantum rings (QRs) grown on GaAs are of interest for use in a large range of devices due to their unusual properties.[1] These nanostructures are type-II, confining holes in a deep potential well,[2] making them candidates for use in novel memories.[3] Their increased carrier recombination time allows them to be used in solar cells, extending the photoresponse into the near infrared.[4] Despite their type-II nature, GaSb/GaAs QD/QRs have also demonstrated potential for use as single photon sources[5] and in light emitting diodes and lasers operating in the 1260–1675 nm telecommunications band.[6–8] Such wavelengths have been difficult to achieve with other GaAs based devices. However, optimal exploitation of the properties of GaSb/GaAs nanostructures in such applications requires an improved understanding of the physics, which is different to that of conventional type-I nanostructures.[9,10] Theoretical studies have demonstrated the importance of understanding the Coulomb interaction of electrons and holes in this system,[11,12] whilst experimental investigations have further illustrated the crucial role played by the strength of electron-hole binding[13] in determining the QD/QR emission wavelength[14,15] and intensity.[16]

Here, we discuss the optical properties of GaSb QRs embedded within a GaAs/$Al_xGa_{1-x}As$ quantum well (QW) in order to determine their viability for use in the active region of vertical cavity surface emitting laser devices.[17–19] We study the effects of changing QW width, n-type doping concentration, and number of GaSb layers on the QR emission. We find that the photoluminescence (PL) emission intensity and energy, and the carrier lifetime are all remarkably resistant to alteration. Only the 5-nm quantum-well sample showed any significant deviation, with a 30 meV increase in emission energy and 28 ± 5% decrease in carrier lifetime. These results testify to the strength of the Coulomb interaction between "free" electrons and confined holes, and corroborate our previous assertion that the QRs must be multiply charged with holes for efficient light emission to occur.[16]

II. EXPERIMENTAL DETAILS

Three distinct types of sample were grown, as shown in Table I: **A** samples with a single QR layer in the centre of a QW with differing widths [Fig. 1(a)], **B** samples with a single QR layer in the centre of a 50 nm QW with different levels of n-type doping, and **C** samples with multiple QR layers in a 100 nm QW [Fig. 1(b)]. All of the GaSb QR samples were grown by molecular beam epitaxy on 2 inch n-type GaAs wafers. First, a GaAs buffer layer was grown at 570 °C followed by 200 nm of $Al_{0.6}Ga_{0.4}As$. Next, the QW regions, which contain the QR layers, were grown. The compositions of this region varied between samples and are shown in Table I and Fig. 1. The 2.1 monolayer (ML) GaSb layer(s) which forms the QRs is common between samples and was deposited at 480 °C, with a growth rate of 0.3 MLs^{-1}. The remaining GaAs in the QWs was deposited at 570 °C, with the exception of the 5 nm immediately above the QR layers,

TABLE I. Summary of the QW regions for each sample.

	QW width (nm)	Doping (cm^{-3})	Number of QR layers
A-5	5	…	1
A-10	10	…	1
A-20	20	…	1
A-50	50	…	1
A-100	100	…	1
A-Ref	…	…	1
B-50n	50	2×10^{16}	1
B-50n+	50	2×10^{17}	1
C-×3	100	…	3
C-×6	100	…	6

a)Electronic mail: pdhodgson@hotmail.co.uk

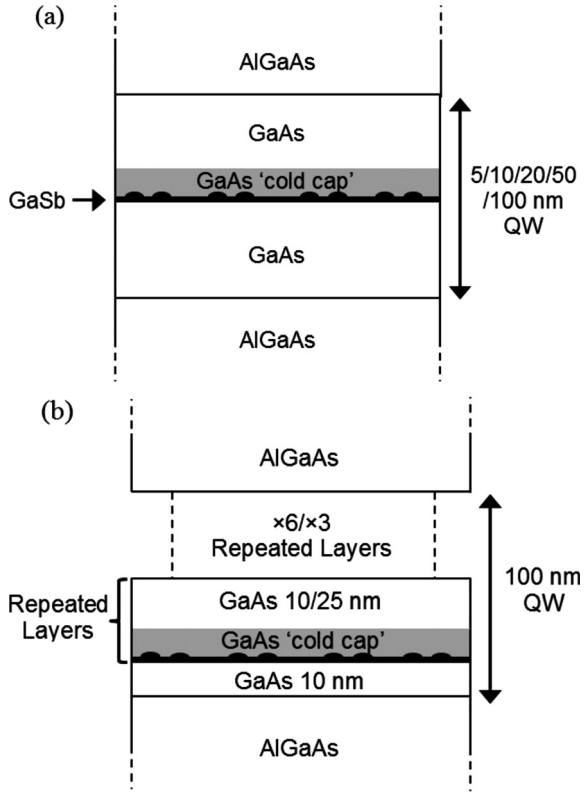

FIG. 1. Schematic diagrams of sample structures. (a) Samples A-5 to A-100, which have different well widths, and (b) samples C-×3 and C-×6, which contain multiple QR layers.

called the "cold cap," which was deposited at 440 °C. This method is known to form QRs during the capping process.[20] The cold cap in sample A-5 is only 2.5 nm thick to allow a total well thickness of 5 nm. A final sample, A-Ref, was grown with identical growth conditions to the other samples, but without the $Al_{0.6}Ga_{0.4}As$ layers, i.e., without a QW. Beam-exit Ar-ion cross-sectional polishing and scanning probe microscopy on an angled sample cross-section[21] was used to measure the thickness of the various layers. All of the layers were found to be their intended thicknesses.

Despite the samples containing a mixture of both QRs and QDs, previous investigations have shown that the QRs are stronger radiative recombination centres and contribute the majority of PL emission.[14,22,23] Thus, we will refer to the 0-D nanostructure PL signal as QR emission for the remainder of this manuscript.

PL measurements were carried out using a 532-nm laser to illuminate the sample via a 200-μm-core optical fibre. An excitation power density of $\sim$30 W/cm^2 was used for all measurements. A 550-μm-core optical fibre collected the PL emission and delivered it to a spectrometer and Peltier-cooled InGaAs array detector. Measurements were carried out in an Oxford Instruments helium-cooled cryostat, which allowed the sample temperature to be varied from 5 to 400 K. Time resolved PL (TRPL) decays were measured using a time-correlated single-photon-counting setup with a FluoTime300 spectrometer and a photomultiplier with a spectral range from 950 nm to 1400 nm. The samples were photoexcited using a 640-nm picosecond pulsed diode operated at a 40-MHz-pulse repetition rate. Bursts of multiple pulses were employed to improve signal sensitivity, allowing high signal recovery from the long lifetime samples. The emission from the samples was collected at right angles to the excitation laser beam at 1220 nm with a spectral bandwidth of 5 nm. The full width at half maximum of the system's instrument response function was 175 ps. The TRPL decay curves were analysed using the FLUOFIT software based on two-exponential models which involves an iterative re-convolution process.[24]

III. RESULTS

We begin our discussion of the results with the **A** samples. These contain a single QR layer in a GaAs/$Al_{0.6}Ga_{0.4}As$ QW. Since the holes are strongly confined in the deep GaSb QR potential well, the effect of changing the well width on the confined hole energy states should be minimal. In contrast, the electrons are unconfined but bound to the QRs by the Coulomb interaction. Therefore, decreasing the QW width should increase the electron energy levels, blueshifting the QR emission. Single-particle simulations using nextnano software[25] were used to model the effect of QW width on the confinement and recombination energies of the QRs. The 3D simulations used the 6-band **k**.**p** method to calculate the hole energy levels and a single-band effective-mass approximation to calculate the electron energy levels. The effects of strain were included in the simulation, and the temperature was set to 300 K. The unstrained GaSb/GaAs valence band offset used in the model is 570 meV at 300 K. The unstrained 300-K band-gaps for GaSb and GaAs are 0.726 eV and 1.422 eV, respectively. The model consisted of a GaAs/$Al_{0.6}Ga_{0.4}As$ QW containing a single GaSb square ring [Fig. 2(a) inset] with inner diameter of 18 nm, outer diameter of 26 nm, and height of 2 nm. These dimensions are similar to those typically found in capped GaSb/GaAs nanostructures.[20] Such nanostructures are roughly circular but often highly disordered,[26] therefore the square shape used in the model is an approximation of the nanostructure geometry, but is expected to be sufficient for the purposes of the simulation. Importantly, the simulation does not include Coulomb effects, which are known to play a significant role in the behaviour of this type-II system. This allowed us to determine the contribution of Coulomb interactions by comparing differences between the model and the PL data from the sample.

Output from the model is shown in Fig. 2(a), with the energies of interest illustrated in the bandgap diagram of Fig. 2(b). It can be seen that the hole energy level, E_h, only has a very weak dependence on well width, as expected due to the very deep hole confining potential of GaSb in GaAs. In contrast, the electron energy level has a strong QW width dependence, and this causes a commensurate dependence for the carrier recombination energy. Therefore, if the electron is unbound or weakly bound to the holes in the QRs, i.e., if the Coulomb binding energy is much less than the electron confinement energy, E_e, the sample data should replicate the simulation data. However, if the electron is tightly bound, the effects of reducing the well width should not be as pronounced as in the simulation.

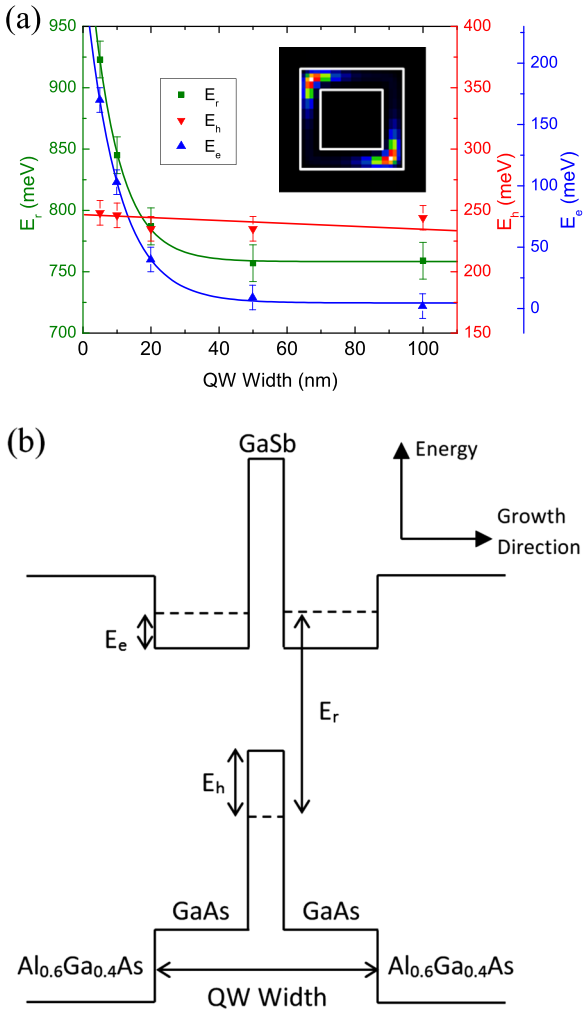

FIG. 2. (a) Carrier energy levels (E_e and E_h) and recombination energies (E_r) predicted by the nextnano simulation. Fitted curves are a guide to the eye. The inset shows the shape of the GaSb nanostructure used in the simulation. The coloured regions show the heavy-hole ground-state probability amplitude. (b) Schematic band-gap diagram of the modelled system with the electron energy level, E_e, the heavy-hole energy level, E_h, and the carrier recombination energy, E_r, labelled.

The PL results for the **A** samples are shown in Fig. 3. PL emission could be seen for all samples up to the 400 K limit of our equipment, demonstrating the potential of these QRs in optical devices. Three distinct emission peaks were observed at low temperature [Fig. 3(a)]. Two of these peaks blue-shifted with increasing excitation power (not shown) and were identified as originating from the QRs and wetting layer (WL), respectively.[9,27] A third peak did not show strong dependence of emission energy on excitation power and is related to carrier recombination in the GaAs substrate.[22] No GaAs QW PL was observed, which is consistent with the very deep hole confining potential of GaSb QRs.[2] It can be seen in Fig. 3(b) that the QR emission energies are the same, within the scatter of the data, for all samples except A-5, which had the narrowest QW. This contrasts with the results of the nextnano simulation, which predicted a clear increase in QR emission energy with well widths below 50 nm [Fig. 2(a)]. Also, within the scatter of the data, all of the samples with well widths greater than 5 nm have identical emission energies to sample A-Ref, which does not contain a QW. We can therefore conclude that the electrons that are radiatively recombining in the QRs experience an intrinsic confinement from Coulomb attraction to holes, which is equivalent to a sub-10-nm QW. Such an effect has previously been predicted by self-consistent calculations.[12] There is also evidence that the geometry of the QRs may enhance this Coulomb effect by allowing electrons to sit in the GaAs-rich ring centres,[14] maximising their proximity to the holes.

The emission energies predicted by the model are systematically lower than those seen in the experiment. Again, this is due to the exclusion of Coulomb effects from the model. It has previously been reported that the characteristic blueshift with increasing excitation density seen in GaSb/GaAs QRs comes primarily from capacitive charging.[15] This causes a ~24 meV increase in emission energy for each subsequent hole added to the QR after the first. Samples grown previously in our laboratory have displayed charge quantised states, which showed that the average charge occupancy of the QRs at low temperatures is 5–6 holes[14] at laser power densities similar to those used in this investigation. Adding this additional energy ($24\,\text{meV} \times (5.5-1) = 108\,\text{meV}$) to the model data shifts the predicted emission energies closer to the experimental values. For example, the model predicts a recombination energy in the 5 nm QW sample of 0.92 eV. Adding the 108 meV capacitive charging energy brings this predicted value to 1.03 eV, which is very close to the experimentally observed value of 1.07 eV at 300 K in Fig. 3(b). The model may also be slightly underestimating the emission energy as a continuous ring was used, rather than smaller disordered structures which are present in the samples.

The QW width also had no observable effect on the emission intensity of the samples, as shown in Fig. 3(c). Moreover, the PL intensity from sample A-Ref with no QW is comparable to the other samples, demonstrating that it is the holes in the QRs, and not the $Al_xGa_{1-x}As$ barriers that is preventing electron escape. Room-temperature TRPL decay traces for all of the samples can be fitted using two distinct lifetimes. It can be seen in Fig. 3(d) that these values, along with the average carrier lifetime, are unchanged (within the scatter of the data) for all well widths other than 5 nm, which showed a $28 \pm 5\%$ shorter lifetime. This indicates an increased electron-hole wave-function overlap, due to the confining effect of the QW, only occurs for the narrowest QW, consistent with the PL energy data. We do not see any difference in PL intensity for the 5-nm QW, but this is dependent on a number of factors, and the reduction in lifetime is modest. The measured lifetimes for all QW widths are longer than has previously been reported for similar zero-dimensional GaSb nanostructures.[12,28] An investigation by Lin *et al.*[28] of single layer and stacked GaSb QRs observed an order of magnitude increase in lifetime, along with a simultaneous increase in emission intensity of two orders of magnitude, for the stacked GaSb QRs sample. This shows that huge variations in recombination dynamics are not unusual in this system, the likely cause being the presence, or lack of, processes that compete with the desired radiative recombination channel.[28] We believe that the long carrier lifetimes in our samples are the result of weak competing

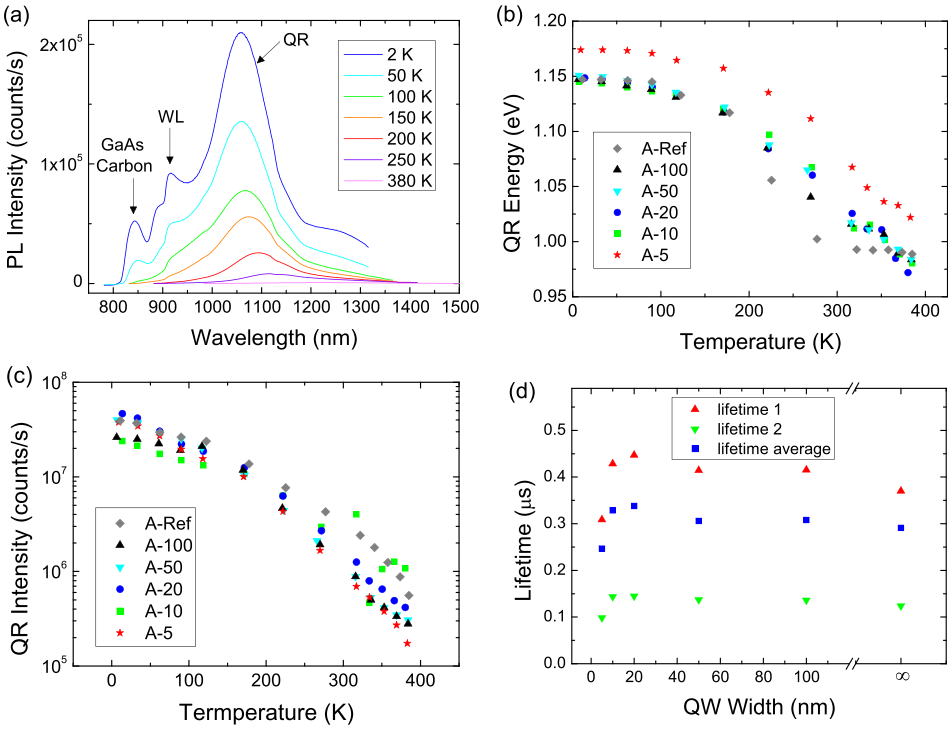

FIG. 3. PL measurements on samples with different QW widths as a function of temperature. (a) Emission spectra of sample A-5 with the QR, wetting layer (WL), and GaAs carbon impurity peak. (b) QR emission energy and (c) integrated QR emission intensity. (d) Carrier lifetimes from TRPL measurements at 300 K.

carrier-recombination processes: at room temperature, the PL from the QRs is the only emission that is observed.

Next, we investigated the effects of doping on the QR PL emission characteristics. Two samples, B-50n and B-50n+, were grown. These samples are identical to A-50, but contain n-type doping of the GaAs in the 50 nm QW. Previous studies have shown that unintentional carbon background doping introduces additional holes into the samples[16,22] and that the average hole occupancy of the QRs is 4 at the lowest PL excitation powers.[14] These additional charge carriers can strongly influence the behaviour of the sample[22] and blueshift the QR emission energy.[15] Hence, if the QR occupancy is dependent on the doping levels in the sample, intentional incorporation of n-type dopants may discharge the QRs and shift their emission energy to longer wavelengths. A simple calculation using an estimated QR density of $3 \times 10^{10}\,\mathrm{cm}^{-2}$ reveals that a n-type doping concentration of $\sim 2 \times 10^{16}\,\mathrm{cm}^{-3}$ in the 50 nm GaAs well is required to give 4 additional electrons per QR and hence counteract the effects of background p-doping. This is the doping level used in sample B-50n. Sample B-50n+ used an order of magnitude higher doping level in order to investigate the effects of excessive doping. If the n-type doping is successful in discharging the QRs of holes, it might be expected that this will reduce the emission intensity and/or energy of the nanostructures, due to a reduction of Coulomb binding of the electrons and capacitive-charging energy of the holes, respectively. It has already been shown, during the investigation of samples A-5 to A-100, that a 50-nm well is wide enough to have no significant effect on radiative emission. Thus, the use of this QW width in the **B** samples should leave the electrons in the vicinity of the QRs unperturbed, allowing the effects of doping to be clearly discerned.

The PL results for these three samples are shown in Fig. 4. It can be seen that there is no clear dependence of either emission energy [Fig. 4(a)] or intensity [Fig. 4(b)] on doping level. This null result is nonetheless interesting. As was previously discussed, charging of these type-II QRs with

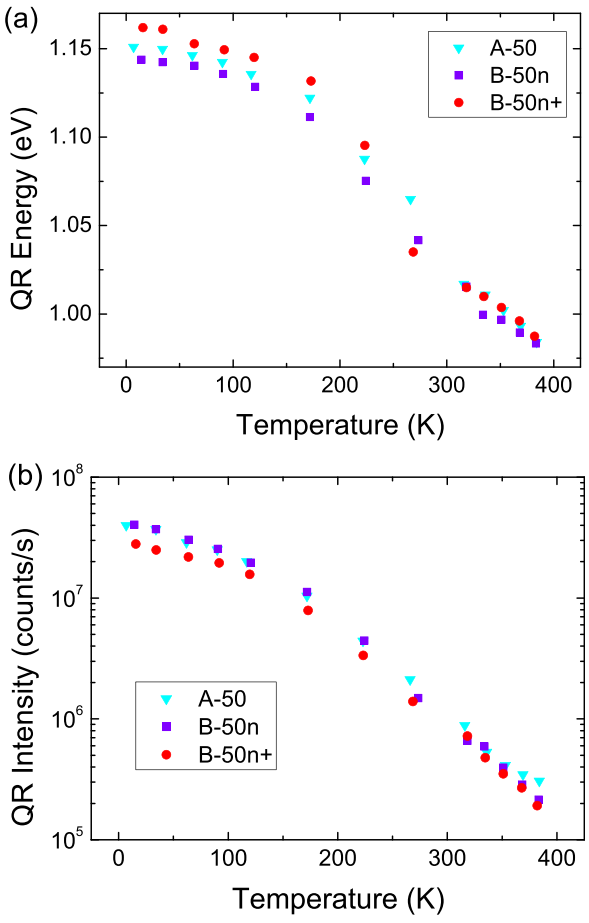

FIG. 4. PL measurements on samples with different n-type doping as a function of temperature. (a) QR emission energy and (b) integrated QR emission intensity.

holes is crucial in determining their PL emission properties. Capacitive charging, due to the spatial separation of electrons and holes, blueshifts the emission energy of the QRs with increasing hole occupancy. We can reasonably assume that the n-type doping of samples B-50n and B-50n+ has counteracted the background p-type carbon dopants which are unavoidably incorporated into the samples. Therefore, the uniformity of emission energies seen in Fig. 4(a) indicates that the QR occupancy is remarkably resilient to doping and carrier concentrations in their local environment. This can be explained by considering the carrier recombination rate of QRs with different hole occupancies.[22] A highly charged QR will strongly bind electrons in its vicinity, giving a high carrier recombination rate, preventing an increase in average QR occupancy. In contrast, a QR charged with fewer holes will bind electrons less strongly, will have a lower recombination rate, and will charge up over time until it reaches a steady state. It does not appear to matter whether these holes come from dopants or photogeneration; the QRs always reach the same hole occupancy, as demonstrated by the nearly identical emission energies and intensities of Fig. 4. In other words, the QR occupancy is self-limiting and our results indicate that it always converges to a similar value, which depends on the recombination mechanics rather than sample doping. This result supports the conclusions of a previous investigation where background dopants were passivated by hydrogenation.[16]

To investigate this self-limiting effect further, a series of 300 K TRPL measurements were made on sample A-50 at different energies across the QR emission peak (Fig. 5). Assuming a charging energy of 24 meV per additional hole,[14] the measured energy range corresponds to a change in QR occupancy of roughly 9 holes. Across this energy range, the average carrier lifetime only changes by roughly 15%, which is orders of magnitude smaller than expected[11,12] and, at first glance, seems to contradict our explanation of self-limiting QR charging. However, the saturation of the average carrier lifetime at lower energy (fewer holes per QR) indicates that a competing (non-radiative) process is dampening the variation

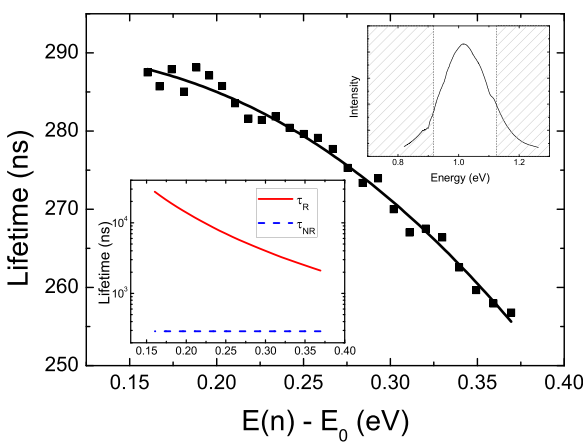

FIG. 5. TRPL average carrier lifetimes for sample A-50 at different energies across the QR emission peak. The fitted curve is a fit to Eq. (1). The upper right inset shows the QR emission peak, with the energy range where lifetimes were measured highlighted. The lower left inset shows the lifetimes extracted from the fitted curve shown in the main figure.

in average carrier lifetime across the emission peak. In other words, a competing short-lifetime non-radiative process is contributing more strongly to the average carrier lifetime than the radiative recombination. A simple lifetime equation

$$\frac{1}{\tau} = \frac{1}{\tau_R(n)} + \frac{1}{\tau_{NR}}, \tag{1}$$

was used to verify this observation. τ is the average carrier lifetime, $\tau_R(n) = A(E(n) - E_0)^x$ is the radiative lifetime, and $E(n)$ is the QR emission energy, which is linearly proportional to the QR occupancy, n.[15] E_0 is the minimum QR emission energy, i.e., the emission energy when the QR is occupied by a single hole. x is a constant which describes the relationship between lifetime and emission energy, τ_{NR} is the lifetime of a competing (non-radiative) process, which is assumed to be invariant with emission energy, and A is a constant.

By fitting Eq. (1) to the experimental data, the values of the lifetimes were determined (Fig. 5) and are plotted in the lower inset to Fig. 5. It can be seen that the radiative lifetime is in the μs range and varies by approximately an order of magnitude across the PL peak. The lifetime for the non-radiative process is shorter than that of the radiative process, supporting our previous assertion that the low-energy saturation observed in Fig. 5 is caused by a competing process. This result also explains why the relative change in average lifetime [Fig. 5 (main figure)] is much smaller than expected—the non-radiative process, which is independent of $E(n)$, contributes much more strongly to the average carrier lifetime, diluting the $E(n)$ dependence of the radiative term. This suggests that even the modest change in average carrier lifetime seen in Fig. 5 is sufficient to provide the dynamic self-limiting charging of QRs we proposed to explain the results of samples A-50, B-50n, and B-50n+.

The emission intensity, $I = 1/\tau_R$, is commonly related to n through the use of the bimolecular rate equation[29]

$$I = bn^2, \tag{2}$$

where b is the bimolecular recombination coefficient. A previous investigation[15] concluded that the bimolecular rate equation was overly simplistic for type-II GaSb/GaAs QRs, and the exponent in Eq. (2) was found to be greater than 2 for all the samples investigated. The fitting function used in Fig. 5 yielded an exponent, x, of -2.6 ± 0.2. Since $(E - E_0) \propto n$, the fitted data suggest that the correct form of Eq. (2) for sample A-50 is $I = bn^{2.6}$, which is consistent with the findings of Ref. 15. Further study of the TRPL as a function of temperature can be expected to reveal deeper insights, but is beyond the scope of the present investigation.

The final part of this investigation looked at the effects of multiple QR layers on emission energy and intensity. Samples C-×3 and C-×6, which contain three and six QR layers, respectively, in a 100 nm QW, were compared with sample A-100. A 100-nm QW was used for two reasons. First, such a wide well should not, and does not, have a noticeable effect on the QR emission properties, as discussed above. Second, it allowed an appreciable number of QR

layers to be grown with sufficient GaAs spacer layers to prevent vertical alignment of nanostructures in successive layers.[30]

It can be seen in Fig. 6(a) that the emission energies of samples of the single and triple QR layers samples, A-100 and C-×3, are almost indistinguishable over the entire temperature range. Only the six layer sample, C-×6, shows any deviation, with roughly a 6 meV reduction in emission energy at temperatures below 150 K. This could result from the increased number of QRs present in the sample, reducing the average QR occupancy, but the reduction in energy is modest and assuming a charging energy of 24 meV per additional hole per QR, corresponds to just 0.25 fewer holes per QR. It is likely that this small decrease in energy results from subtle variations in the nanostructure morphology between samples. This supports the earlier conclusion from the **B** samples that the QRs must be sufficiently charged in order for carriers to recombine efficiently, and this minimum charge level appears consistent across samples, as indicated by the almost identical emission energies.

The emission intensity for the samples shown in Fig. 6(b) appears to only be modestly affected by layer number. The intensity data contain jumps as the temperature changed, which we attribute to small but unavoidable movements of the optical fibre during measurements. Regardless of these uncertainties, the intensity clearly does not show a proportional dependence on the number of QR layers. The lower temperature data points contain less scatter and are best for use in an intensity comparison. The six layer sample, C-×6, is only twice as intense as the single layer sample, A-100, at 10 K. A similar sub-linear increase in intensity with layer number has been observed previously in GaSb/GaAs QR samples.[31] We cannot conclusively explain why this is the case, but it is very likely that the laser power density used in our experiment is not high enough to exploit the additional QR layers.

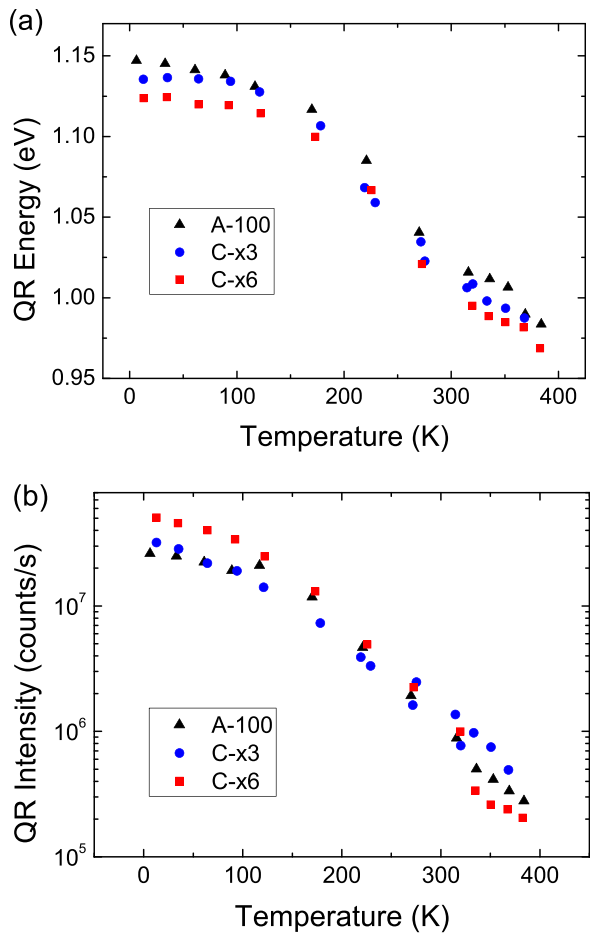

FIG. 6. PL measurements on samples with different numbers of GaSb QR layers as a function of temperature. (a) QR emission energy and (b) integrated QR emission intensity.

IV. CONCLUSIONS

We have investigated the effects of QW layer thickness, n-type doping, and multiple QR layers on the PL emission of GaSb/GaAs QRs. It was found that decreasing the well width has a remarkably small effect on QR emission energy and intensity. This shows that the strength of the "confinement" of electrons by Coulomb attraction to holes in the QRs is equivalent to a sub-10-nm QW. The results of adding n-type doping to the GaAs around the QRs revealed that multiple hole occupancy of the QRs is required for efficient carrier recombination, regardless of whether these holes come from doping or excitation. Finally, an investigation into the effect of multiple QR layers indicated that high excitation powers may be required to fully exploit the benefits to emission intensity from additional layers.

ACKNOWLEDGMENTS

The authors would like to thank Dr. Andrew Marshall of Lancaster University for providing useful information and advice on molecular beam epitaxy. This work was supported by the Engineering and Physical Sciences Research Council [Grant No. EP/M50838X/1]. The data for this manuscript are openly available from the Lancaster University data archive at DOI: 10.17635/lancaster/researchdata/16.

[1]M. Hayne *et al.*, J. Phys. D: Appl. Phys. **46**, 264001 (2013).
[2]T. Nowozin *et al.*, Appl. Phys. Lett. **102**, 052115 (2013).
[3]A. Marent, T. Nowozin, M. Geller, and D. Bimberg, Semicond. Sci. Technol. **26**, 014026 (2011).
[4]R. B. Laghumavarapu, A. Moscho, A. Khoshakhlagh, M. El-Emawy, L. F. Lester, and D. L. Huffaker, Appl. Phys. Lett. **90**, 173125 (2007).
[5]M. P. Young *et al.*, AIP Adv. **4**, 117127 (2014).
[6]J. Tatebayashi, A. Khoshakhlagh, S. H. Huang, G. Balakrishnan, L. R. Dawson, and D. L. Huffaker, Appl. Phys. Lett. **90**, 261115 (2007).
[7]W. H. Lin, K. W. Wang, S. Y. Lin, and M. C. Wu, IEEE Photonics Technol. Lett. **25**, 97 (2013).
[8]T. H. Loeber, D. Hoffmann, and H. Fouckhardt, Beilstein J. Nanotechnol. **2**, 333 (2011).
[9]B. Bansal, S. Godefroo, M. Hayne, G. Medeiros-Ribeiro, and V. V. Moshchalkov, Phys. Rev. B **80**, 205317 (2009).
[10]B. Bansal, M. Hayne, M. Geller, D. Bimberg, and V. V. Moshchalkov, Phys. Rev. B **77**, 241304(R) (2008).
[11]K. Gradkowski, T. J. Ochalski, D. P. Williams, S. B. Healy, J. Tatebayashi, G. Balakrishnan, E. P. O'Reilly, G. Huyet, and D. L. Huffaker, Phys. Status Solidi B **246**, 752 (2009).
[12]K. Gradkowski, T. J. Ochalski, N. Pavarelli, H. Y. Liu, J. Tatebayashi, D. P. Williams, D. J. Mowbray, G. Huyet, and D. L. Huffaker, Phys. Rev. B **85**, 035432 (2012).
[13]M. Ahmad Kamarudin, M. Hayne, R. J. Young, Q. D. Zhuang, T. Ben, and S. I. Molina, Phys. Rev. B **83**, 115311 (2011).

[14]R. J. Young, E. P. Smakman, A. M. Sanchez, P. Hodgson, P. M. Koenraad, and M. Hayne, Appl. Phys. Lett. **100**, 082104 (2012).
[15]P. D. Hodgson, R. J. Young, M. Ahmad Kamarudin, P. J. Carrington, A. Krier, Q. D. Zhuang, E. P. Smakman, P. M. Koenraad, and M. Hayne, J. Appl. Phys. **114**, 073519 (2013).
[16]P. D. Hodgson, M. Hayne, M. Ahmad Kamarudin, Q. D. Zhuang, S. Birindelli, and M. Capizzi, Appl. Phys. Lett. **105**, 081907 (2014).
[17]E. Soderberg, J. S. Gustavsson, P. Modh, A. Larsson, Z. Z. Zhang, J. Berggren, and M. Hammar, J. Lightwave Technol. **25**, 2791 (2007).
[18]J. Jewell, L. Graham, M. Crom, K. Maranowski, J. Smith, T. Fanning, and M. Schnoes, Phys. Status Solidi C **5**(9), 2951 (2008).
[19]M. C. Amann and W. Hofmann, IEEE J. Sel. Top. Quantum Electron. **15**, 861 (2009).
[20]E. P. Smakman, J. K. Garleff, R. J. Young, M. Hayne, P. Rambabu, and P. M. Koenraad, Appl. Phys. Lett. **100**, 142116 (2012).
[21]A. J. Robson, I. Grishin, R. J. Young, A. M. Sanchez, O. V. Kolosov, and M. Hayne, ACS Appl. Mater. Interfaces **5**, 3241 (2013).
[22]P. D. Hodgson, R. J. Young, M. Ahmad Kamarudin, Q. D. Zhuang, and M. Hayne, Phys. Rev. B **88**, 155322 (2013).
[23]M. Hayne, J. Maes, S. Bersier, V. V. Moshchalkov, A. Schliwa, L. Muller-Kirsch, C. Kapteyn, R. Heitz, and D. Bimberg, Appl. Phys. Lett. **82**, 4355 (2003).
[24]D. V. Oconnor, W. R. Ware, and J. C. Andre, J. Phys. Chem. **83**, 1333 (1979).
[25]S. Birner, T. Zibold, T. Andlauer, T. Kubis, M. Sabathil, A. Trellakis, and P. Vogl, IEEE Trans. Electron Devices **54**, 2137 (2007).
[26]A. J. Martin *et al.*, Appl. Phys. Lett. **102**, 113103 (2013).
[27]F. Hatami *et al.*, Phys. Rev. B **57**, 4635 (1998).
[28]W. H. Lin, K. W. Wang, S. W. Chang, M. H. Shih, and S. Y. Lin, Appl. Phys. Lett. **101**, 031906 (2012).
[29]E. F. Schubert, *Light-Emitting Diodes* (Cambridge University Press, 2003).
[30]N. N. Ledentsov *et al.*, Phys. Rev. B **54**, 8743 (1996).
[31]P. J. Carrington, A. S. Mahajumi, M. C. Wagener, J. R. Botha, Q. Zhuang, and A. Krier, Physica B **407**, 1493 (2012).